Intelligent Automation And Soft Computing, 2020
Vol.26,no.4,643–661
DOI: 10.32604/iasc.2020.010100

A Multi-objective Invasive Weed Optimization Method for Segmentation of Distress Images

Eslam Mohammed Abdelkader[1, 2], Osama Moselhi[3], Mohamed Marzouk[4], and Tarek Zayed[5]

[1]Ph.D. candidate, Department of Building, Civil, and Environmental Engineering, Concordia University, Montreal, QC, Canada.
[2]Assistant lecturer, Structural Engineering Department, Faculty of Engineering, Cairo University, Egypt.
[3]Professor, Department of Building, Civil, and Environmental Engineering, Concordia University, Montreal, QC, Canada.
[4]Professor, Structural Engineering Department, Faculty of Engineering, Cairo University, Egypt.
[5]Professor, Department of Building and Real Estate, the Hong Kong Polytechnic University, Hung Hom, Hong Kong.

ABSTRACT
Image segmentation is one of the fundamental stages in computer vision applications. Several meta-heuristics have been applied to solve the segmentation problems by extending the Otsu and entropy functions. However, no single-objective function can optimally handle the diversity of information in images besides the multimodality issues of gray-level images. This paper presents a self-adaptive multi-objective optimization-based method for the detection of crack images in reinforced concrete bridges. The proposed method combines the flexibility of information theory functions in addition to the invasive weed optimization algorithm for bi-level thresholding. The capabilities of the proposed method are demonstrated through comparisons with single-objective optimization-based methods, conventional segmentation methods, multi-objective genetic algorithm-based method, multi-objective particle swarm-based method and multi-objective harmony search-based method. The proposed method outperformed the previously-mentioned segmentation methods, whereas the average values of mean-squared error, peak signal to noise ratio and structural similarity index are equal to 0.0784, 11.4831 and 0.9921, respectively.

KEYWORDS: Image segmentation, meta-heuristics, multimodality, multi-objective optimization, crack, reinforced concrete bridges, invasive weed optimization algorithm.

1 INTRODUCTION

BRIDGES are vulnerable to severe deterioration agents, which promote their deterioration agents along their service life. As per the Canadian infrastructure report card, 26% of the bridges are either “Fair”, “Poor” or “Very Poor” (Felio et al., 2016). Moreover, one-third of Canada’s bridges have structural or functional deficiencies with short remaining service life, where 20 million light vehicles, 750,000 trucks, and 15,000 public transits use the Canadian bridges annually (National Research Council Canada, 2013). The average age of the bridges is 24.5 years in 2007 compared to a mean service life of 43.3 years. Thus, 57% of the estimated service life has already been consumed (Statistics Canada, 2009). In addition to that, the backlog of bridge maintenance, rehabilitation and replacement is estimated to be equal to $10 billion. The continuous increase in the backlog results in a significant deterioration in the condition of the bridge elements (Sennah et al., 2011).

Based on the aforementioned statistics, it is very crucial to evaluate the condition of the bridge decks in order to maintain them within a safe condition. Thus, maintenance-related interventions should be condition driven in order to preserve the condition values of the bridges and to ensure the public safety. As such, this paper presents a novel method for the segmentation of cracks in reinforced concrete bridges. Crack is one of the most common concrete defects, whereas their presence leads to the development of other modes of failure. Thus, bridge crack detection is crucial for

CONTACT Eslam Mohammed Abdelkader eslam_ahmed1990@hotmail.com

timely maintenance of various concrete bridges. Recently, the use of digital image processing to deal with the surface defect became a research trend because the accuracy and efficiency of visual inspection-based methods are highly dependent on the skills and experience of inspectors. Thus, the subjectivity associated with the visual inspection-based methods requires the development of an automated method for the detection of cracks. The proposed method aids in improving accuracy, reducing cost and minimizing the inherent subjectivity of the manual inspection. Segmentation is a key stage in the automatic bridge crack detection because the accuracy of the detection and quantification of distresses is highly sensitive to the threshold values used in the segmentation. Accordingly, it is decisive to compute optimal threshold that discriminates between the distressed and non-distressed regions.

The main objectives of the present study are as follows:

1- Review the previously-developed image segmentation methods.
2- Develop a self-adaptive multi-objective invasive weed optimization-based method for bi-level thresholding.
3- Compare the proposed method with other commonly-utilized segmentation methods present in the literature.

2 TYPES OF SEGMENTATION METHODS

IMAGE segmentation is one of the basic and critical operations used to analyze the retrieved images in pattern recognition, geographical imaging and medical imaging applications. Image segmentation is the process of dividing the image into non-overlapping multiple segments based on some attributes such as color, intensity and texture. Thresholding is one of the most frequently utilized image segmentation algorithms, whereas thresholding methods usually define the optimal threshold value based on the maximization and minimization of a single-objective function. Image thresholding can be divided into: bi-level thresholding and multi-level thresholding.

Bi-level thresholding (binarization) is the process of dividing the image into two segments which are: foreground (object of interest) and background. Thus, the main objective of the image segmentation process is to define the optimum threshold that distinguishes the foreground from the background. However, when the thresholding is extended to multi-level thresholding in the case of complex images, multi-level thresholding can serve as a better alternative, which involves utilizing a finite set of threshold values in order to classify the retrieved image into more than two homogenous classes (Akay, 2013). The thresholding process becomes a more exhaustive search process, and consequently, the computational time increases exponentially by increasing the number of threshold values.

There are basically two approaches to handle the optimal thresholding problems which are: parametric and non-parametric approaches. For the parametric approaches, the gray-level of each class is assumed to follow a probability density function, normally a Gaussian probability density function is assumed. Then, the statistical parameters of each class are computed. The least-squared method can be used as one of the algorithms to estimate the parameters of the distribution that best-fits the gray-level histogram, leading to a non-linear optimization problem (Hammouche et al., 2008). However, the parametric approaches are computationally exhaustive and the performance is highly dependent on the initial conditions (Akay, 2013). The non-parametric approaches tend to find the optimal thresholds that partition the gray-level regions based on some discriminating criteria such as Renyi entropy, cross entropy and the between-class variance (Otsu's function) (Zhang and Wu, 2011).

3 LITERATURE REVIEW

PREVIOUS segmentation methods are based on extending information theory functions such as cross entropy and Tsallis entropy or Otsu function by employing evolutionary algorithms. Many meta-heuristic optimization algorithms were introduced in the last few years to search for the optimum thresholds because of the computational inefficiency of conventional search methods. This section provides an overview of the different image segmentation methods present in the literature.

3.1 Entropy-based Methods

Agrawal et al. (2013) proposed an approach to search for the optimal threshold values of multi-level thresholding by the maximization of Tsallis entropy using cuckoo search mechanism. They concluded that the cuckoo search algorithm outperformed other meta-heuristic algorithms such as bacteria foraging optimization algorithm, artificial bee colony optimization algorithm, particle swarm optimization algorithm, and genetic algorithm in terms of processing time and accuracy. In another study, Suresh and Lal (2017) presented an approach for multi-level thresholding of satellite images based on Tsallis entropy and minimum cross entropy as objective functions. They utilized chaotic Darwinian particle swarm optimization (CDPSO) algorithm to search for the optimal threshold values. They illustrated that CDPSO outperformed cuckoo search algorithm, harmony search algorithm, differential evolution algorithm and particle swarm optimization algorithm based on some performance metrics such as peak signal to noise ratio (PSNR), mean-squared error (MSE), structure similarity index (SSIM) and the computational time.

Manic et al. (2016) employed the firefly algorithm for multilevel thresholding based on the maximization

of Tsallis entropy and Kapur entropy. They concluded that Kapur entropy-based approach provided faster convergence and lower processing time. However, Tsallis entropy-based approach provided better segmentation quality. Sathya and Kayalvizhi (2011) proposed a bacterial foraging optimization (BFO)-based cross entropy approach for multi-level thresholding. They highlighted that BFO offered higher peak signal to noise ratio when compared to the particle swarm optimization algorithm and genetic algorithm.

3.2 Otsu-based Methods

Aziz et al. (2017) applied two swarm optimization algorithms, namely whale optimization (WO) algorithm and moth-flame optimization (MFO) algorithm for multi-level thresholding. The objective was to search for the optimum threshold values that maximize the Otsu's function. They highlighted that for a higher number of thresholding problems, the MFO algorithm achieved higher fitness function values, PSNR and SSIM when compared to the WO algorithm. Nevertheless, the MFO algorithm required longer computational time to search for the optimal values. Banharnsakun (2017) developed an image segmentation method that integrates artificial bee colony algorithm and Otsu function for the pavement surface distress detection. The introduced method provided better segmentation results when compared to the differential evolution algorithm, artificial bee colony algorithm, genetic algorithm, and Ostu function

3.3 Entropy and Ostu-based Methods

Khairuzzaman and Chaudhury (2017) employed grey wolf optimization (GWO) algorithm for multi-level thresholding based on Kapur entropy and Otsu functions. They concluded that the proposed method provided better quality results when compared to particle swarm optimization algorithm and bacterial foraging optimization algorithm. However, GWO provides slower convergence than PSO algorithm and faster convergence than BFO algorithm. Mishra and Panda (2018) applied bat algorithm for multi-level color thresholding of Lena image. They investigated different objective functions based on accuracy and processing time such as Tsallis entropy, Kapur entropy, Shannon entropy, Renyi entropy, and Otsu. They highlighted that Otsu function provided good segmentation results in addition to the fast convergence when compared to the entropy functions.

3.4 Other Segmentation Methods

Ganesh et al. (2017) introduced an enhanced adaptive K-means clustering method to improve the segmentation of Magnetic Resonance Imaging (MRI) of the brain. The segmentation method was based on applying the opening morphological operation on the output of the K-means clustering method to enhance the segmentation performance. The proposed method achieved better segmentation capability when compared to the adaptive K-means clustering method and fuzzy C-means clustering method. Nandy et al. (2015) presented an enhanced-based clustering method to improve the segmentation process through the application of cuckoo search algorithm. The cuckoo search algorithm was utilized to minimize the sum of squared Euclidean distance between the cluster centers and the patterns with a certain cluster. The cuckoo search algorithm achieved better color segmentation performance when compared to the genetic algorithm, dynamic control particle swarm optimization algorithm and firefly algorithm.

Hu (2012) utilized fuzzy C-means clustering algorithm for the segmentation of crop nutrient deficiency. Median filter was applied as a pre-processing stage to remove noise from the image. The proposed method outperformed other segmentation methods such as threshold method, edge detection method and domain division method. Hooda et al. (2014) investigated the performance of K-means clustering algorithm, fuzzy C-means clustering algorithm and region growing algorithm in the segmentation of brain tumor in the MRI images. The quantitative analysis was conducted based on 10 MRI images; whereas they highlighted that the fuzzy C-means clustering algorithm outperformed other segmentation methods based on the error percentage. Khanna et al. (2012) utilized a combination of expectation maximization algorithm and Gabor filter for the segmentation of ultrasound images. The image was divided into multi-resolutions that were consistent to different texture characteristics based on orientation angle of 30º. Then, the expectation algorithm was applied to the filtered images. The proposed method achieved more satisfactory segmentation results when compared to the K-means clustering algorithm.

3.5 Research Gaps

Conventional image segmentation methods include Otsu, region growing, K-means clustering, etc. The main limitation of the conventional exhaustive methods is their inefficiency as a search mechanism in the case of higher complex images, which causes them to be a less credible segmentation method, and subsequently leading to poor segmentation results. Thus, the bio-inspired computing paradigms can serve as a better search mechanism to find the optimal threshold values based on a pre-defined objective function.

Most reported research utilizes single-objective optimization problems to search for the optimal thresholds in the images. Nonetheless, there is no single thresholding objective function, which can optimally fit all types of images, i.e., produces an optimum threshold for all types of images. Therefore, a multi-objective optimization problem is designed in this paper using a combination of objective functions

in order to improve the performance of the image segmentation process. Some gray level histograms of some images are unimodal. Nevertheless, some are multimodal. Solving multimodal search spaces are very complex and exhaustive task to be achieved. The multimodality of the histograms makes it exhaustive for the optimization algorithm to find the optimum solution much more than the unimodal histograms. Therefore, an efficient optimization algorithm has to be developed to explore the multimodal search spaces. Therefore, the main objective of the present study is to develop a self-adaptive multi-objective optimization-based method that deploys a set of information theory functions as well as invasive weed optimization algorithm for bi-level thresholding.

4 PROPOSED METHOD

THE framework of the proposed methodology is depicted in Figure 1. The primary objective of the present study is to design a self-adaptive method that delineates the segmentation process of cracks in reinforced concrete bridges. This includes designing an exhaustive search multi-objective optimization method to optimize the threshold values and to explore the effectiveness of its application when compared to other segmentation methods. In the present study, bi-level thresholding is applied to segment the crack images by employing invasive weed optimization algorithm. The objective of the bi-level thresholding is to generate a single threshold T that classifies the image pixels into two classes: the foreground (distress) and background (surface). The thresholding function is described in Equation 1.

$$G(x,y) = \begin{cases} 1, if\ F\ x,y) \geq T \\ 0\ , otherwise \end{cases} \quad (1)$$

where $G(x,y)$ represents the binary image. $F\ x,y)$ represents the gray image. T denotes the threshold that separates the foreground from the background, whereas if the image pixels are above the threshold, they are appended to the foreground otherwise, they are appended to the background.

Image segmentation methods can be divided into five main categories which are: 1) edge detection-based methods, 2) clustering-based methods, 3) region-based methods, 4) histogram-based methods, and 5) optimization-based methods. In the recent years, image segmentation problems are modeled as optimization problems, whereas the optimum threshold is computed based on a predefined objective function such as maximizing of the between-class variance, maximization of the Kapur entropy, and minimization of the Bayesian error.

The optimization-based methods provide more accurate results when compared with other image segmentation methods especially in the complex images (non-uniform illumination images). However, it requires more computational effort. Thus, the optimization-based methods used in the module are dedicated to the classification and quantification of the surface defects. The detection of surface distresses is a challenging task that requires a high level of accuracy for two main reasons: 1) existence of low contrast between the cracks and surrounding deck area, inhomogeneity of intensity and presence of shadows of similar intensity to the cracks. These conditions imply the existence of multimodal search spaces, and 2) higher potential of inaccurate segmentation, which results in imprecise extraction of the parameters of the surface defects, which subsequently lead to inaccurate classification and quantification of the surface defects. The implication of small differences in the threshold values of the extracted parameters (length, width, area) further substantiate the use of the optimization-based methods in the developed module

The framework of the present study investigates more than one objective function to enable the assessment of different types of images. Each one of them has its own assumption, and therefore it fits only a certain kind of images. The proposed method investigates five objective functions which are: maximization of Kapur entropy, maximization of Tsallis entropy, maximization of Renyi entropy, minimization of cross entropy, and maximization of the between-class variance (Otsu function) for the inclusion of the best performing functions in the subsequent phase. As shown in Figure 1, the proposed image segmentation method is divided into two phases: PHASE I and PHASE II. For PHASE I, five methods are investigated to solve the image segmentation problem by finding the optimum thresholds of the images. The optimum threshold is computed based on the five methods stated above. The proposed method utilizes the invasive weed optimization algorithm to find the optimum solutions (thresholds) based on each objective function separately.

Then, the five image segmentation methods are ranked based on three performance indicators which are: mean-squared error, peak signal to noise ratio and structural similarity index. These indicators are used to automatically analyze the performance of segmentation methods. Subsequently, the best two performing image segmentation methods are selected to be used to design a bi-objective optimization problem. The best two performing objective functions are the ones which achieved the lowest mean-squared error, highest peak signal to noise ratio and highest structural similarity index. In PHASE II, The multi-objective optimization problem is also solved using the same optimization algorithm and the same initial setting of parameters in PHASE I in order to provide an equal basis of comparison.

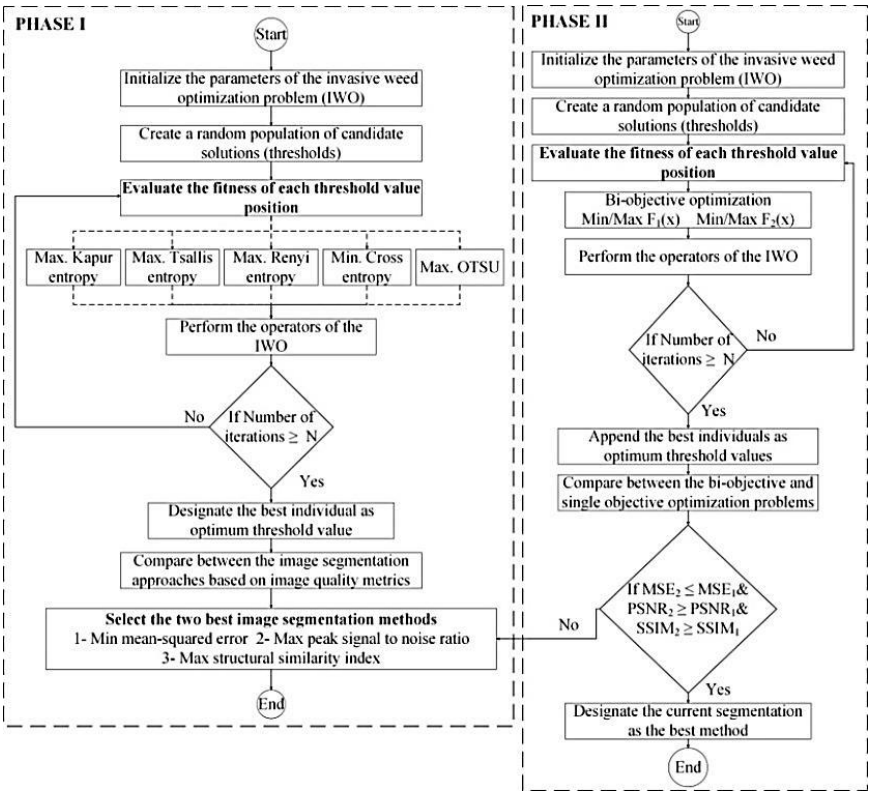

Figure 1. Framework of the Proposed Image Segmentation Method.

The results obtained from the bi-objective optimization model are compared with the results of the single-objective optimization methods (best two segmentation methods). If there is an improvement, the current design of the bi-objective optimization model is appended and will be utilized for the subsequent steps. If not, the best method obtained from PHASE I, is utilized instead. The proposed method (multi-objective invasive weed optimization-based method) is validated through detailed levels of comparisons with single-objective optimization-based methods, some commonly utilized image segmentation methods and a set of metaheuristic algorithms using a diverse set of test images. The image segmentation methods are: Otsu method, K-means clustering, region growing, fuzzy C-means clustering, expectation maximization and adaptive thresholding. The metaheuristic algorithms include: genetic algorithm, particle swarm optimization algorithm and harmony search algorithm. This comparison enables to demonstrate the robustness of the proposed method, non-dependency towards the kind of image and applicability to be applied to a wide range of images.

5 BI-LEVEL THRESHOLDING

THE objective of the multi-objective optimization problem is to find the threshold that optimizes the best two performing objective functions obtained from PHASE I. Due to the paper size limitations, two of the previously-mentioned five segmentation methods is described in the following lines. More details about other segmentation methods can be found in Khairuzzaman and Chaudhury (2017), and Mishra and Panda (2018).

5.1 Cross Entropy Method

Cross entropy is known as "Divergence", which is an information metric that is used to measure the distance between two probability distributions. Assume $A = \{A_1, A_2, A_3, A_4, \dots\dots A_N\}$ and $B = \{B, B_2, B_3, B_4, \dots\dots B_N\}$, which represent two probability distributions. The cross entropy between A and B can be computed using Equation 2 (Horng 2010; Oliva et al., 2019).

$$D(A,B) = \log \sum_{i=1}^{N} A_i \left(\frac{A_i}{B_i}\right) \qquad (2)$$

where $D(A,B)$ represents the cross entropy between the two probability distributions.

The minimum cross entropy thresholding (MCET) algorithm is based on finding the optimum threshold T between the original image of the segmented image. Assume an image I that contains L gray-levels $\{0, 1, 2, 3, \dots\dots L-1\}$. Then, the segmented image I_t obtained based on the threshold T can be defined using the following Equation.

$$I_t\,(x,y) = \begin{cases} \mu(0, T-1), if\ I\ \ x,y) < T \\ \mu\ \ T, L-1), if\ I\ \ x,y) \geq T \end{cases} \quad (3)$$

The normalized value of the cross entropy between the ranges c and d can be computed using Equation 4.

$$\mu(c,d) = \frac{\sum_{i=c}^{d-1} iH(i)}{\sum_{i=c}^{d-1} H(i)}\ , i = 0, 1, 2, 3, \dots\dots L-1 \quad (4)$$

The minimum cross entropy thresholding algorithm finds the optimum threshold by minimizing the cross entropy of the image (objective function) as shown in Equation 5.

$$D(T) = \min\left[\sum_{i=1}^{L} ih\ \ i) \times log(i) - \sum_{i=1}^{t-1} ih\ \ i) \times log\big(\mu\ \ 1,\ t)\big) - \sum_{i=t}^{L} ih\ \ i) \times log\big(\mu\ \ t,\ L)\big)\right]$$

Since the first term is constant for a given digital image, the objective function can be re-formulated as follows.

$$D(T) = \min\left[-\sum_{i=1}^{t-1} ih\ \ i) \times log\big(\mu\ \ 1,\ t)\big) - \sum_{i=t}^{L} ih\ \ i) \times log\big(\mu\ \ t,\ L)\big)\right] \quad (6)$$

where

$$D(T) = \min\left[-\sum_{i=0}^{T-1} i \times h(i) \times log\ \ \frac{\sum_{i=0}^{T-1} i \times h(i)}{\sum_{i=0}^{T-1} i \times h(i)}) - \sum_{i=T}^{L-1} \mathrm{i} \times \mathrm{h(i)} \times \log\left(\frac{\sum_{i=T}^{L-1} \mathrm{i} \times \mathrm{h(i)}}{\sum_{i=T}^{L-1} \mathrm{i} \times \mathrm{h(i)}}\right)\right] \quad (7)$$

5.2 Otsu Method

Otsu method was proposed by Otsu, which is an un-supervised algorithm that is used to segment an image by maximizing the variance between the segmented classes. Assume an image I that contains L gray-levels $\{0, 1, 2, 3, \dots\dots L-1\}$. The cumulative probabilities of the segmented classes can be computed using Equation 8. The mean values of the segmented classes can be calculated using Equation 9 (Khairuzzaman and Chaudhury, 2017; Mishra and Panda, 2018).

$$W_1 = \sum_{i=0}^{T-1} p_i\ , W_2 = \sum_{i=T}^{L-1} p_i \quad 8)$$

$$\mu_1 = \sum_{i=0}^{T-1} \frac{i \times P_i}{W_1}, \mu_2 = \sum_{i=T}^{L-1} \frac{i \times P_i}{W_1} \quad 9)$$

where W_1 and W_2 denote the cumulative probabilities for the classes C_1 and C_2, respectively. μ_1 and μ_2 denote the cumulative probabilities for the classes C_1 and C_2, respectively.

The variances of the segmented classes can be computed using Equations 10 and 11.

$$\sigma_1{}^2 = \ W_1 \times \ \mu_1 - \mu_t)^2 \ (10)$$

$$\sigma_2{}^2 = \ W_2 \times \ \mu_2 - \mu_t)^2 \ (11)$$

Give that:

$$\mu_t = \ \ W_1 \times \mu_1) + \ W_2 \times \ \mu_2) \quad (12)$$

where $\sigma_1{}^2$ and $\sigma_2{}^2$ denote the variances of C_1 and C_2, respectively. μ_t denotes the total cumulative probabilities.

Therefore, the objective of the optimization problem is to find the gray threshold T, which maximizes the following objective function (class variances).

$$F(T) = \max(\sigma_0{}^2 + \sigma_1{}^2) \ (13)$$

5.3 Invasive Weed Optimization Algorithm

Invasive weed optimization (IWO) is a meta-heuristic bio-inspired optimization algorithm that was developed by Mehrabian and Lucas in 2006. IWO is based on simulating the invasive behaviour of weed in colonizing and finding the most suitable place for growth and reproduction. Weeds are robust and undesirable plants that grow spontaneously and they can have a harmful effect on both farms and gardens (Abu-Al-Nadi et al., 2013). The flowchart of the invasive weed optimization algorithm is illustrated in Figure 2.

The first step is to create an initial population of weeds that are spread in the i-dimensional search space. The fitness of each weed within the population is calculated based on a predefined objective function. The production of seeds associated with each weed is calculated based on a linear function, where the number of seeds varies between the minimum and maximum number of seeds. Each weed in the population produces seeds based on its own comparative fitness value, maximum and minimum fitness values within the population, and the maximum and minimum number of seeds. The reproduction of seeds is shown in Equation 14 where the higher the fitness of the weed, the more seeds it produces (Zhou and Xidan, 2014; Azizipour et al., 2016).

$$Seed_i = \frac{f_i - f_{min}}{f_{max-f_{min}}} \times \ s_{max} - s_{min}) + s_{min} \quad (14)$$

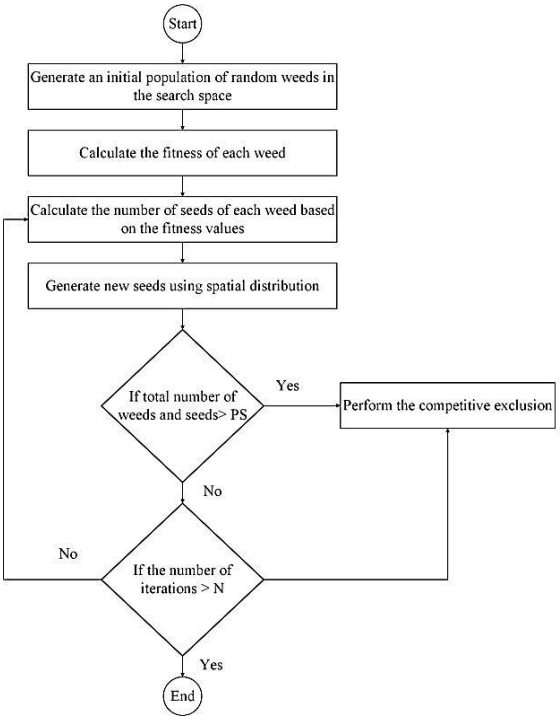

Figure 2. Flowchart of the Invasive Weed Optimization Algorithm.

Where $Seed_i$ represents number of seeds associated with the $i-th$ weed. f_i represents the current fitness of the weed. f_{max}, and f_{min} represent the maximum and minimum fitness of the current population, respectively. s_{max}, and s_{min} denote the maximum and minimum number of seeds, respectively.

The next step is the spatial dispersion, where the seeds are randomly scattered in the search space based on a normal distribution of a mean equal to zero and an adaptive varying standard deviation. This step ensures that the seeds are accumulated around the weed plant, which leads to a local search around each parent weed. The standard deviation of the seed dispersion is reduced from an initial predetermined maximum value to an initial predetermined smaller value based on a non-linear function as shown in Equation 15. The probability of finding a seed far from the weed plant is high at the beginning of the optimization process and it decreases within a predefined number of iterations (Azizipour et al., 2016).

$$\sigma_i = \sigma_{min} + \left(\frac{iter_{max} - iter}{iter_{max} - iter_{min}}\right)^p \times \sigma_{max} - \sigma_{min}) \quad (15)$$

where σ_i indicates the standard deviation of the current iteration. σ_{max}, and σ_{min} indicate the initial and final standard deviation of the optimization process, respectively. $iter_{max}$ represents the maximum number of iterations. p represents non-linear modulation index, and usually, it is a number between two and three.

Finally, competitive exclusion is performed because the number of weeds and seeds reaches the maximum population size due to the fast reproduction (exponential increase in the number of plants). The parent weeds along side with the seeds are ranked based on the fitness value in order to eliminate the solutions with the least fitness values to keep the number of the weed plants and seeds within the maximum allowable population size. The seeds and their parent weeds with higher fitness survive, and become reproductive. The process continues until the convergence criteria are satisfied (reaching the maximum number of iterations). Code is written in order to employ the invasive weed optimization using Matlab R2013a. More details about the genetic algorithm and particle swarm optimization algorithm can be adopted from Mohammed Abdelkader et al. (2019) while more information about the harmony search algorithm can be found in Oliva et al. (2013).

6 CONVENTIONAL IMAGE SEGMENTATION METHODS

THIS section provides an overview of some of the conventional image segmentation methods that the proposed method is compared with, in order to demonstrate the capabilities of the proposed method.

6.1 Region-based Methods

Region-based methods are based on mapping the image into a set of connected pixels called “Regions” based on a predefined homogeneity criterion. Then, the groups of pixels are grouped into larger regions based on this attribute. The region grows until no more neighbouring pixels can be added. Then, a new seed pixel is selected from the unlabeled pixels and the process continues until all the pixels present in the image are labeled. Region-based methods can be divided into region growing methods, and region splitting and merging methods. The present study utilizes region growing method because it is considered as one of the most commonly utilized region-based methods, which proved its capability in providing an accurate segmentation of the image. Region growing methods are based on agglomerating neighbouring pixels that can maintain the homogeneity of the region.

The indicator of homogeneity is based on estimating the average intensity and standard deviation to grow the area. This homogeneity indicator is used to express the uniformity or non-uniformity of the image pixels of a connected region. The homogeneity indicator is sometimes referred to as “logical predicate”. The neighboring pixels are added to the region if the indicator of homogeneity is true and the growth stops until no more neighbouring pixels can be added to the region without violating the

homogeneity. The three main factors of the growing region method are as follows: 1) selection of the initial seed points, 2) definition of the homogeneity criterion, and 3) definition of the stopping criterion. The formulation of the segmentation process based on the region-based method is to divide an image I to N number of regions from R_i to R_N based on a logical predicate P. The main steps of the region growing are depicted in the following Equations (Saparudin et al., 2018; Maru and Shah, 2013).

$$I = \bigcup_{i=1}^{N} R_i \quad (16)$$

$$R_i \text{ is a connected region}, i = 1, 2, 3, \dots\dots\dots N \quad (17)$$

$$R_i \bigcap R_j = \phi, for\ all\ i\ and\ j, i \neq j \quad (18)$$

$$P(R_i) = \text{TRUE}, for\ all\ i = ,2,3, \dots\dots\dots N \quad (19)$$

$$P(R_i \bigcup R_j) = \text{FALSE, for any adjacent regions: } R_i\ and\ R_j \quad (20)$$

6.2 Clustering-based Methods

Clustering is an unsupervised algorithm, which is used to divide the image into segments that contain pixels of similar characteristics. Clustering-based methods select the optimal threshold by dividing the image into object and background. There are two types of clustering algorithms which are: 1) hard clustering algorithms and 2) soft clustering algorithms. Hard clustering is a clustering algorithm; whereas the image is divided into clusters so that an image pixel belongs to only one cluster, i.e., hard clustering algorithms utilize membership function values of zero or one. Thus, the image pixel can belong to a cluster or not. The present study investigates K-means clustering algorithm, which is one of the most commonly used hard clustering algorithms. In the soft clustering algorithms, the image pixel belongs to more than one cluster based on the degree of membership. Two soft clustering algorithms are investigated which are: fuzzy C-means and expectation maximization (Shedthi et al., 2017; Kaur and Kaur, 2014).

6.2.1 K-means clustering

K-means clustering algorithm is based on minimizing the distance between the average squared Euclidean distance between the data points and the clusters' centroids. The main distinct feature between K-means and K-medoids clustering algorithms is that one of the data points represents the centroid of the cluster in the case of k-medoids. K-means algorithm utilizes the mean of the data points. The steps of K-means clustering algorithm are as follows (Sawant, 2015):

1- Select the number of desired clusters K.
2- Select K starting points randomly to be used as initial candidates for clusters' centroids.
3- Calculate the distance between data points and cluster centroids.
4- Assign the data point to the cluster centroid which has the minimum distance between the data point and cluster centroids. The distance is simply the Euclidean distance.

$$d(x_i, C_j) = \sqrt{\sum_{d=1}^{n} (x_{id} - c_{id\,i})^{\,2}} \quad (21)$$

5- Re-compute the new cluster centroids (centroid is the mean point of the cluster).
6- Repeat steps 3, 4, and 5 until convergence (centroid and data points no longer move).

6.2.2 Fuzzy C-means clustering

Fuzzy C-means clustering (FCM) is an iterative clustering algorithm where each data point is assigned to one cluster or more based on the membership degrees. FCM was developed by Dunn in 1973 and improved by Bezdek in 1981. FCM is based on minimizing the following objective function (Keskin, 2015).

$$J_w = \sum_{i=1}^{N} \sum_{j=1}^{C} u_{ij}^{m} \left|\left|(X_i - C_j)^2\right|\right| \quad (22)$$

where m is a fuzzifier constant that is greater than one. u_{ij} denotes the degree of membership of the X_i in the cluster j and it is between zero and one. X_i is a $i-th$ data point in a d-dimensional space. C_j represents the centroid of the $j-th$ cluster. $||*||$ is a norm distance that represents the similarity between the data point and the centroid of the cluster.

FCM starts by randomly initiating the cluster centroid. The second step is to construct the membership matrix. A membership matrix ($U_{(N\times C)}$) is composed of a group of membership degrees. The degree of membership (u_{ij}) can be calculated using Equation 23. The cluster centroids are then updated and can be calculated using Equation 24. The cluster centroids and the membership degrees are iteratively updated until the convergence criteria are satisfied. The convergence criteria is shown in Equation 25. The de-fuzzification process is performed using Equation 26 such that the data point is assigned to the cluster that has the maximum degree of membership.

$$u_{ij} = \frac{1}{\sum_{k=1}^{C} \left(\frac{\left|\left|(X_i - C_j)\right|\right|}{\left|\left|(X_i - C_k)\right|\right|} \right)^{\frac{2}{m-1}}} \quad (23)$$

$$C_j = \frac{\sum_{i=1}^{N} u_{ij}^{m} \times X_i}{\sum_{i=1}^{N} u_{ij}^{m}} \quad (24)$$

$$\max_{ij}\{|u_{ij}^{it+1} - u_{ij}^{it}|\} < \zeta \quad (25)$$

$$D_j = \arg_i\{max(u_{ij})\} \quad (26)$$

$$\sum_{j=1}^{c} u_{ij} = 1 \quad (27)$$

where D_j represents the de-fuzzified value, which is calculated based on the maximum degree of membership principle. ζ is the termination constant between zero and one. it refers to the number of iteration steps.

6.2.3 Expectation maximization

The expectation maximization clustering algorithm calculates the probabilities of cluster memberships based on one or more probability distribution. The number of the clusters is predetermined in the expectation maximization algorithm. Expectation maximization algorithm is based on maximizing the probability that the data point belongs to the clusters of the model. The expectation maximization clustering algorithm utilizes Gaussian Mixture Models (GMM). Expectation maximization algorithm starts by calculating the membership degree of each point in the cluster, then the mixture model parameters are updated, then the process continues until the stopping criteria is satisfied (Jung et al., 2014).

7 PERFORMANCE METRICS

THREE indicators are used to evaluate the quality of the segmented images, which are: mean-squared error (MSE), peak signal to noise ratio ($PSNR$) and structural similarity index ($SSIM$). Image quality indicators provide an automatic judgment to reflect the quality of segmented images instead of evaluating the segmentation process through human eye perception. These indicators compare between the image segmentation methods based on the image intensity values. Structural similarity index combines luminance comparison, contrast comparison and structural comparison. Mean-squared error, peak signal to noise ratio and structural similarity index can be obtained using Equations 28, 29 and 30, respectively. An efficient image segmentation method is the one, which achieves the lower MSE, higher $PSNR$ and higher $SSIM$ (Suresh and Lal, 2017; Mishra and Panda, 2018; Chakraborty et al., 2017).

$$MSE = \frac{1}{m \times n}\sum_{i=1}^{m}\sum_{j=1}^{n}[\ X(i,j) - Y(i,j)]^2 \quad (28)$$

$$PSNR = 10 \times \log_{10}\left(\frac{R^2}{MSE}\right) \quad \text{(in dB)} \quad (29)$$

$$SSIM = \frac{(2\mu_x\mu_y + C1) \times (2\sigma_{xy} + C2)}{(\mu_x^2 + \mu_y^2 + C2) \times\ \sigma_x^2 + \sigma_y^2 + C2)} \quad 30)$$

Give that:

$$C1 = \ K_1 \times L)^2 \quad (31)$$

$$C2 = \ K_2 \times L)^2 \quad (32)$$

where $X(i,j)$ and $Y(i,j)$ represent the original and segmented image, respectively. R denotes the maximum intensity value in the original image. σ_{xy} denotes the covariance of the images X and Y. L represents the number of gray levels. K_1 and K_2 represent two constants, which are equal to 0.01 and 0.03, respectively.

8 MODEL IMPLEMENTATION

TWENTY distress images are utilized as an input to evaluate the performance of the image segmentation algorithms. These images are captured from three bridge decks in Montreal and Laval, Canada using Sony DSC-H300 digital camera of 20.1 megapixel resolution. The first step is to convert the true-color image RGB (red green and blue) to the grayscale image. The images have a size of 400×400. Samples of the distress images are shown in Figure 3. The digital images are prone to degradation by noise during the image acquisition phase or during unfavourable conditions during image transmission. These conditions can substantially affect the subsequent image processing phases such as image segmentation and feature extraction. Thus, the image restoration should be performed before other image processing phases take place. The image restoration aims at removing the maximum noise from the degraded image while preserving the important features in the image. Wiener filer is a frequency domain filter, which means that it utilizes discrete Fourier transform (DFT) to transform the degraded image to the frequency domain. The proposed method utilizes Wiener filter of size 5×5 to suppress the variations in illumination (non-uniform illumination), enhance the contrast and remove the noise in images.

The concrete crack images are characterized by some attributes: 1) different types of cracks such as vertical crack, horizontal crack and alligator crack, 2) different orientations for the different types of cracks, 3) different lighting conditions and 4) complex background components. These four attributes enable to investigate the efficiency and robustness of the proposed method. In order to differentiate between the conventional Otsu method and Otsu method based on the single-objective optimization problem. The conventional Otsu method is referred to as “Otsu I” while the Otsu method based on the optimization problem is referred to as “Otsu”. The performed analysis is a four-tier comparison in order to demonstrate the capabilities of the proposed method. The first stage is to compare the proposed multi-objective optimization-based method with the single objective-based optimization methods. The second stage is to compare the proposed method with the

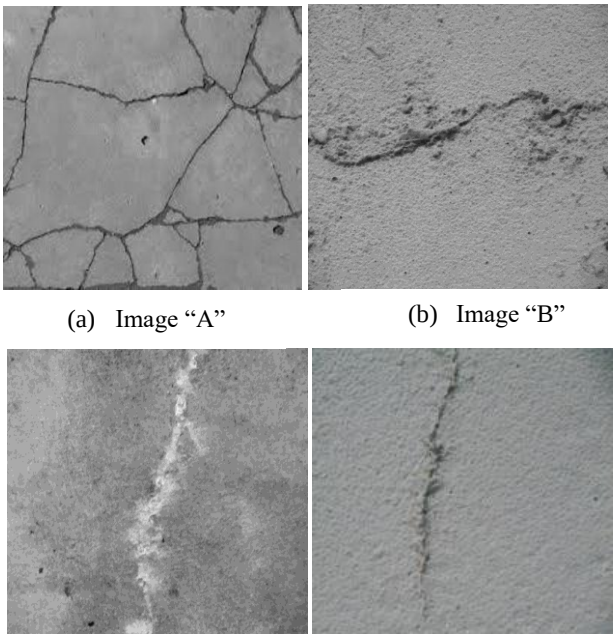

(a) Image "A" (b) Image "B"

(d) Image "C" (c) Image "D"

Figure 3. Sample of the Distress Images.

segmentation methods present in the literature. The third stage is to validate the utilization of the invasive weed optimization algorithm. The last stage is to investigate the performance of the proposed method for a specific number of images to ensure its consistent superior performance. To compare between the segmented (thresholded) images, mean-squared error, peak signal to noise ratio and structural similarity index are used as quality diagnostics to evaluate the optimum threshold values and consequently the segmented images. These quality diagnostics assess the similarities between the segmented image and the original image. All the calculations and optimization algorithms took place on a laptop with an Intel Core i7 CPU, 2.2 GHz and 16 GB of memory.

The first stage is to compare between the five fitness functions which are: Kapur entropy, Tsallis entropy, Renyi entropy, cross entropy, and Otsu method. Invasive weed optimization algorithm is utilized to find the optimum threshold that separates the distress from the background. The parameters of the invasive weed optimization algorithm are listed in Table 1. In order to provide a comprehensive overview of the segmentation performance and to design the bi-objective optimization problem, a comparison is conducted between the five optimization methods for the whole twenty images. The performances of the five optimization-based methods for the whole images are depicted in Table 2. The values of the performance indicators listed in Table 2 represent the average performance indicators. It is worth mentioning that, the differences in the values of the performance indicators are not significant because the segmentation methods are dealing with binary images. Kapur entropy function and Renyi entropy function provided the better performance while the performance of Otsu method was the least. Average values of MSE, $PSNR$ and $SSIM$ of the Renyi entropy are equivalent to 0.0974, 11.2289 and 0.9898, respectively while average values of MSE, $PSNR$ and $SSIM$ of the Kapur entropy are equivalent to 0.1006, 11.0839 and 0.9898, respectively. MSE, $PSNR$ and $SSIM$ of the Otsu method are equal to 0.124, 10.0931 and 0.9876, respectively.

Table 1. Parameters of the Invasive Weed Optimization Algorithm.

Parameter of the invasive weed optimization algorithm	Value
Initial population size	10
Maximum number of iterations	20
Minimum number of seeds	0
Maximum number of seeds	5
Initial standard deviation	0.5
Final standard deviation	0.001

Table 2. Performance Comparison between the Different Optimization-based Segmentation Methods.

Method	Average mean-squared error ($AMSE$)	Average peak signal to noise ratio ($APSNR$)	Average structure similarity index ($ASSIM$)
Renyi entropy	0.0974	11.2289	0.9898
Tsallis entropy	0.1054	11.262	0.9879
Kapur entropy	0.1006	11.0839	0.9898
Cross entropy	0.1013	11.1913	0.9898
Otsu method	0.124	10.0931	0.9876
Proposed method	0.0784	11.4831	0.9921

As mentioned before, there is a fundamental rationale that no single objective function can optimally fit all types of images. Thus, a multi-objective optimization model is designed by encompassing the merits of the two best performing single objective functions to produce more consistent and efficient solutions. The parameters of the multi-objective optimization problem are the same as the parameters listed in Table 1 in order to provide an equal basis of comparison. Based on Table 2, the two best performing single objective functions are: Renyi entropy and Kapur entropy. Therefore, the multi-objective optimization problem is formulated by providing a trade-off between Renyi entropy approach and Kapur entropy approach.

To validate the claim that the proposed multi-objective invasive weed optimization-based method can introduce better segmentation process when

compared to the single objective functions, an experiment is conducted to compare between the proposed method and the previously adopted single-objective optimization-based methods in terms of the average values of the MSE, $PSNR$ and $SSIM$. For the proposed method, the average values of the MSE, $PSNR$ and $SSIM$ are equal to 0.0784, 11.4831 and 0.9921, respectively. The experimental results verifies and manifests that the proposed method (multi-objective optimization problem) yields better optimal solutions and better segmentation results when compared to the single-objective optimization methods.

The second stage is to conduct a comparison between the proposed method and other segmentation methods present in the literature as shown in Table 3. Other segmentation methods encompass some algorithms such as clustering-based methods, region growing methods and histogram-based methods. The segmentaion methods include: region growing, K-means clustering, fuzzy C-means clustering, expectation maximization, Otsu I and adaptive thresholding. For instance, based on the K-means clustering the average values of the MSE, $PSNR$ and $SSIM$ are equal to 0.1991, 7.0347 and 0.9681, respectively. Based on the region growing method, the average values of the MSE, $PSNR$ and $SSIM$ are equal to 0.2022, 6.9321 and 0.9652, respectively. The proposed method presents a percentage of improvement for the $AMSE$, $APSNR$ and $ASSIM$ equal to 61.227%, 65.651% and 2.787%, respectively when comapred to the region-growing method. Thus, based on the conducted experiments, the proposed methods significantly outperforms other segmentation approaches, whereas the proposed method introduces the best segmentation followed by Otsu I method then adaptive thresholding method. On the other hand, expectation maximization method provides the least segmentation performance. Otsu I method is considered as the most common method in the segmentation of surface distresses. The proposed method yielded an improvement in the $AMSE$, $APSNR$ and $ASSIM$ by 39.225%, 28.999% and 0.558%, respectively.

A third comparison is conducted in order to validate the proposed method, whereas the performance of the invasive weed optimization algorithm is compared with other commonly utilized metaheuristic algorithms in segmentation. The comparison is conducted for the same benchmark of images in addition to the same population size and number of iterations in order to provide an equal basis of comparison. For the genetic algorithm, tournament selection is the parent selection strategy. Two-point crossover is utilized, and the crossover rate is assumed 0.8. Mutation rate is assumed 0.1. For the particle swarm optimization algorithm, the cognitive learning and social parameters are assumed two while the inertia weight is assumed 0.5. The damping factor of the inertia weight is assumed 0.99. For the harmony search algorithm, the harmony search size is 10. The harmony memory consideration rate and pitch adjustment rate are assumed 0.9 and 0.1, respectively.

Table 3. Performance Comparison between the Different Image Segmentation Methods.

Method	Average mean-squared error ($AMSE$)	Average peak signal to noise ratio ($APSNR$)	Average structure similarity index ($ASSIM$)
Proposed method	0.0784	11.4831	0.9921
K-means clustering	0.1991	7.0347	0.9681
Otsu I method	0.129	8.9017	0.9862
Region growing	0.2022	6.9321	0.9652
Fuzzy C-means clustering	0.1989	7.0898	0.968
Expectation maximization clustering	0.2271	6.7233	0.9638
Adaptive thresholding	0.1508	8.8102	0.9851

Ten different optimization runs are carried out in order to provide a robust comparison between the optimization algorithms. The average computations of the performance metrics for the four metaheuritstics for all images are shown in Table 4. As shown in Table 4, the invasive weed optimization outperformed the other three metaheuristic algorithms, whereas the values of $AMSE$, $APSNR$ and $ASSIM$ are equal to 0.0784, 11.4831 and 0.9921, respectively. On the other hand, the genetic algorithm provided the least performance, whereas the values of $AMSE$, $APSNR$ and $ASSIM$ are equal to 0.099, 11.1705 and 0.9898, respectively. This illustrates the capability of the invasive weed optimization in searching for the optimum threshold that provides the least minimum-squared error, highest peak signal to noise ratio and highest structural similarity index by amplifying the exploration-exploitation trade-off.

A fourth comparison is performance in order to examine the consistency of the proposed method. The proposed method is compared with the conventional segmentation methods for images “A”, “C” and “D” to provide an in-depth evaluation for the segmentation performance of the proposed method. The convergence curve of the Kapur entropy of image “A” is depicted in Figure 4. As shown in Figure 4, the cost function stabilizes after iteration 7, which illustrates the superior search capability of the invasive weed optimization algorithm. The threshold values and the performance of the different optimization-based

Table 4. A Comparative Analysis between a Set of Metaheuristic Algorithms based on Ten Runs for All Images.

Metaheuristic algorithm	Average mean-squared error ($AMSE$)	Average peak signal to noise ratio ($APSNR$)	Average structure similarity index ($ASSIM$)
Invasive weed optimization algorithm	0.0784	11.4831	0.9921
Genetic algorithm	0.099	11.1705	0.9898
Particle swarm optimization algorithm	0.0986	11.3622	0.9899
Harmony search algorithm	0.0992	11.0744	0.9899

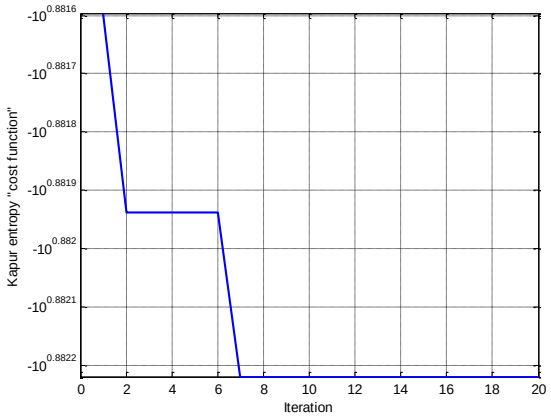

Figure 4. Convergence Curve of the Kapur Entropy Objective Function.

Table 5. Threshold Values, Fitness Function Values and Other Performance Indicators of the Optimization-based Methods for Image "A".

Method	Threshold value (T)	Fitness function value	MSE	$PSNR$	$SSIM$
Renyi entropy	118	7.6503	0.1869	7.2842	0.9815
Tsallis entropy	121	108.0131	0.1866	7.292	0.9819
Kapur entropy	120	7.6246	0.1865	7.294	0.9821
Cross entropy	113	1.3082×10^{5}	0.1876	7.2678	0.9808
Otsu method	150	1.0409×10^{4}	0.312	5.2281	0.9565

Table 6. Performance Comparison between the Different Segmentation Methods for image "A".

Method	MSE	$PSNR$	$SSIM$
Proposed method	0.1865	7.294	0.9921
K-means clustering	0.2013	6.9618	0.981
Otsu I method	0.1874	7.2716	0.9919
Region growing	0.1949	6.3924	0.9898
Fuzzy C-means clustering	0.2013	6.9618	0.981
Expectation maximization clustering	0.2013	6.9618	0.981
Adaptive thresholding	0.1922	6.4534	0.9835

methods for image "A" are shown in Table 5. As shown in Table 5, different thresholds are obtained based on each segmentation methods, whereas Kapur entropy function provides the best performance in terms of MSE, $PSNR$ and $SSIM$ while Otsu method provides the least performance in terms of MSE, $PSNR$ and $SSIM$. MSE, $PSNR$ and $SSIM$ of the Kapur entropy are equal to 0.1865, 7.294 and 0.9821, respectively. MSE, $PSNR$ and $SSIM$ of the Otsu method are equal to 0.312, 5.2281 and 0.9565, respectively.

A comparative analysis of the different segmentation methods for image "A" is described in Table 6. The proposed method achieved very promising results. It achieved the highest accuracy in image segmentation such that the values of MSE, $PSNR$ and $SSIM$ are equal to 0.1865, 7.294 and 0.9921, respectively. Expectation maximization, K-means clustering and fuzzy C-means clustering attained the least accurate segmentation results, whereas the values of MSE, $PSNR$ and $SSIM$ are equal to 0.2013, 6.9618 and 0.981. The gray-level histograms along with the threshold values and segmented images using the proposed method are illustrated in Figure 5. The threshold value is equal to 123. The proposed method provides very efficient segmentation for image "A". A clearer visual comparison is presented between the different segmentation methods, whereas any pixel that has a pixel of value equal to one, is considered as a distress pixel while any pixel that has a value equals to zero, is considered as a non-distress. Figure 6 depicts the segmented images using region growing, Otsu I, K-means clustering and the proposed method. Figure 7 depicts the segmented images using fuzzy C-means clustering, expectaion maxmization and adaptive thresholding. By examining the differences between the segmented images, it is clearly visible that the proposed method yields a superior segmentation performance when compared to other methods.

A performance comparison for image "C" based on the different image segmentation methods is presented in Table 7. The proposed method provided better

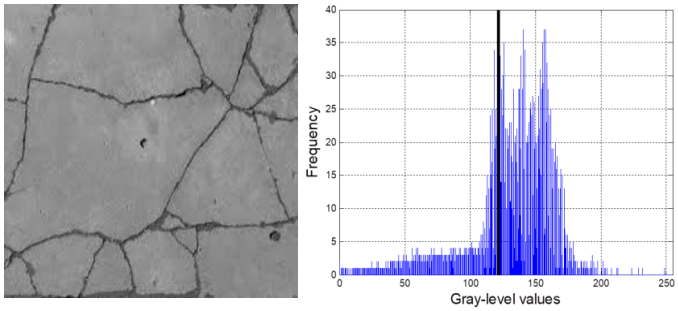

(a) A sample image (b) Gray-level histogram with the threshold

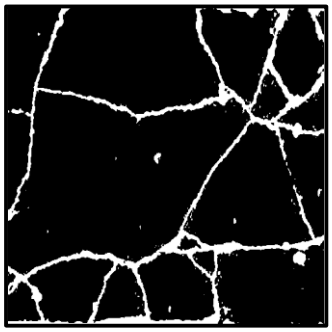

(c) Segmented image

Figure 5. A Sample of the Input Images, their Associated Gray-level Histograms, Threshold Values and Segmented Images based on the Proposed Method.

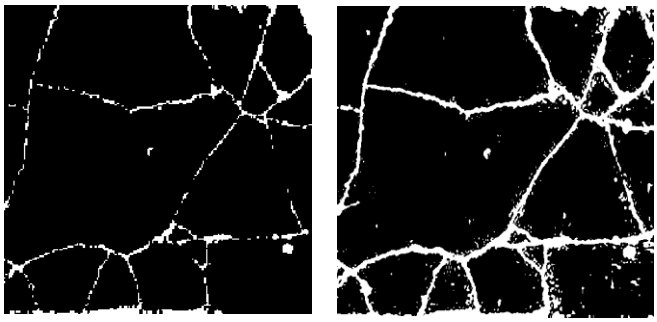

(a) Region growing (b) Otsu I

(c) K-means clustering (d) Proposed method

Figure 6. Image Segmentation for Image "A" using (a) Region Growing, (b) Otsu I, (c) K-means Clustering and (d) Proposed Method.

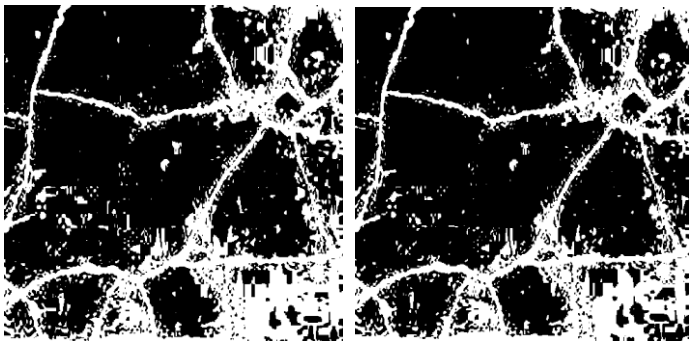

(a) Fuzzy C-means clustering (b) Expectation maximization

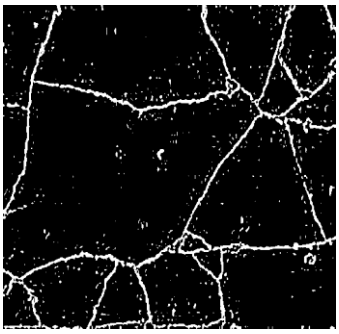

(c) Adaptive thresholding

Figure 7. Image Segmentation for Image "A" using (a) Fuzzy C-means Clustering, (b) Expectation Maximization and (c) Adaptive Thresholding.

Table 7. A Comparative Analysis between the Different Segmentation Methods for Image "C".

Method	MSE	$PSNR$	$SSIM$
Proposed method	0.2158	5.8382	0.9927
K-means clustering	0.3064	4.3164	0.9751
Otsu I method	0.2934	4.5041	0.9754
Region growing	0.238	5.4129	0.9855
Fuzzy C-means clustering	0.3118	4.2406	0.976
Expectation maximization clustering	0.3118	4.2406	0.976
Adaptive thresholding	0.2842	4.6241	0.9752

segmentation capability when compared to other methods present in the literature. The MSE, $PSNR$ and $SSIM$ achieved by the proposed method are equal to 0.2158, 5.8382 and 0.9927, respectively. Region growing method achieved the second best performance such that MSE, $PSNR$ and $SSIM$ are equal to 0.238, 5.4129 and 0.9855, respectively. On the other hand, expectation maximization and fuzzy C-means clustering methods attained the least performance, whereas the MSE, $PSNR$ and $SSIM$ are equal to 0.3118, 0.2406 and 0.976, respectively. The segmentation results obtained from the region growing, Otsu I, K-means clustering, proposed method, fuzzy C-means clustering, expectation maximization, and adaptive thresholding are shown in Figures 8 and 9. As shown in Figures 8 and 9, the segmentation of the crack images is significantly improved by applying the proposed method.

A comparison of the different segmentation methods for image "D" is shown in Table 8. The proposed method had the best segmentation outcome, where the MSE, $PSNR$ and $SSIM$ achieved by the proposed method are equal to 0.2038, 6.0872 and 0.9919, respectively. Otsu I method had the second best performance followed by region growing method. Adaptive thresholding provided the least performance such that the MSE, $PSNR$ and $SSIM$ are equal to 0.2547, 5.118 and 0.9742, respectively. The thresholded images using the different image segmentation methods are depicted in Figures 10 and 11 for a visual understanding for the quality of optimal threshold values. It can be inferred that the proposed

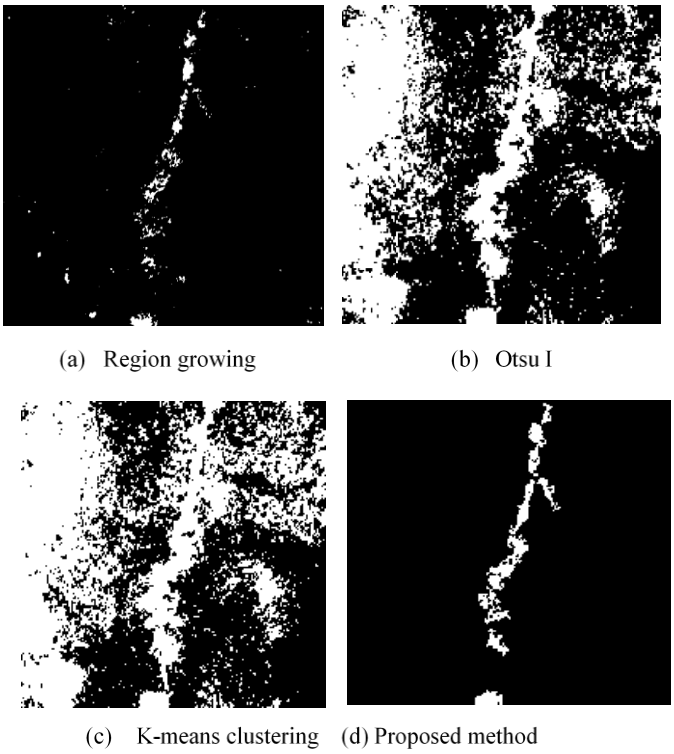

Figure 8. Image Segmentation for Image "C" using (a) Region Growing, (b) Otsu I, (c) K-means Clustering and (d) Proposed Method.

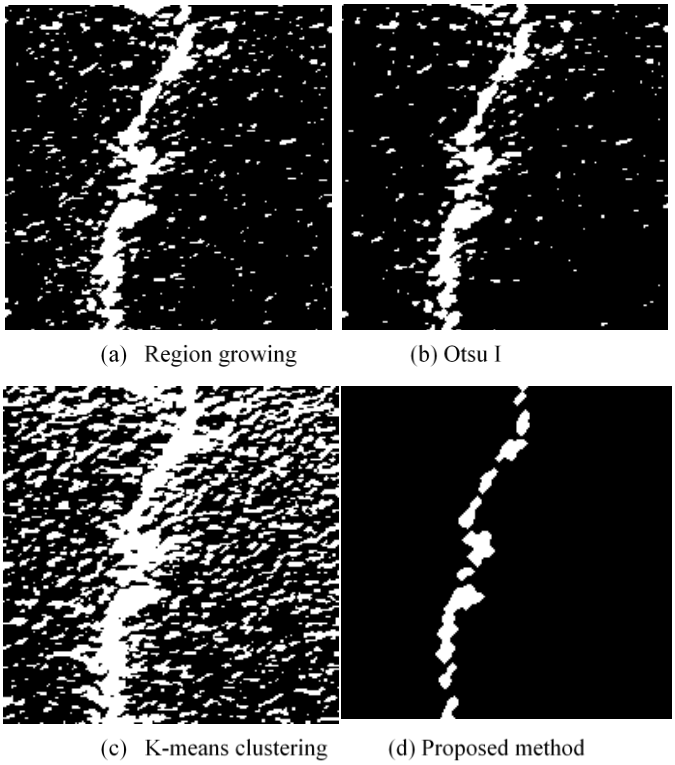

Figure 9. Image Segmentation for Image "C" using (a) Fuzzy C-means Clustering, (b) Expectation Maximization and (c) Adaptive Thresholding.

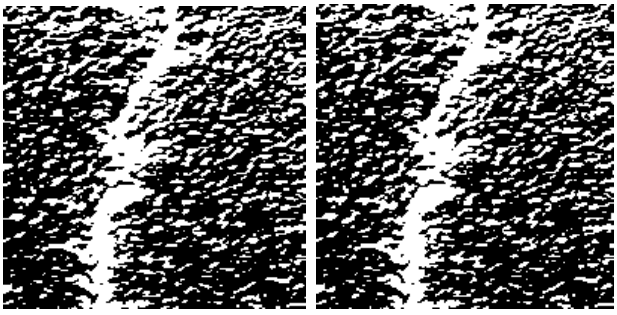

(a) Fuzzy C-means clustering (b) Expectation maximization

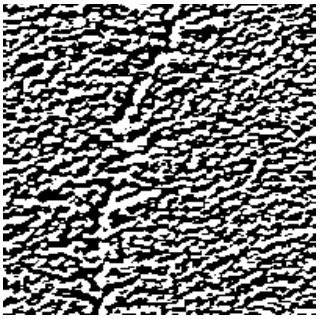

(c) Adaptive thresholding

Figure 10. Image segmentation for image "D" using (a) Region Growing, (b) Otsu I, (c) K-means Clustering and (d) Proposed Method.

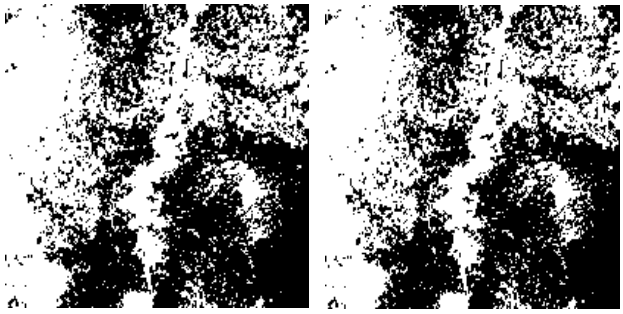

(a) Fuzzy C-means clustering (b) Expectation maximization

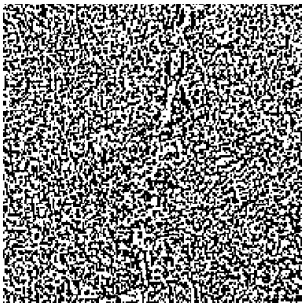

(c) Adaptive thresholding

Figure 11. Image Segmentation for Image "D" using (a) Fuzzy C-means Clustering, (b) Expectation Maximization and (c) Adaptive Thresholding.

Table 8. A Comparative Analysis between the Different Segmentation Methods for Image "D".

Method	MSE	$PSNR$	$SSIM$
Proposed method	0.2038	6.0872	0.9919
K-means clustering	0.2401	5.3745	0.9749
Otsu I method	0.2101	5.9549	0.987
Region growing	0.2138	5.8795	0.985
Fuzzy C-means clustering	0.2401	5.3745	0.9749
Expectation maximization clustering	0.2401	5.3745	0.9749
Adaptive thresholding	0.2547	5.118	0.9742

method has a superior segmentation capability by visually investigating the quality of the thresholded images. Based on the detailed comparisons for images "A", "C" and "D", the proposed method provided a consistent superior segmentation capability than other methods, which aids in overcoming the inconsistency of other segmentation methods. Thus, the self-adaptive multi-objective optimization-based method adopted in the present study is capable of achieving a consistent, robust and remarkable improvement in the segmentation as per the four levels of comparison. The conducted comparisons demonstrate how the proposed method can be effectively deployed in the detection of distresses, which enables constructing more accurate condition assessment models.

9 CONCLUSION

IMAGE segmentation is one of the most critical and basic tasks in image processing because it remarkably affects image feature extraction especially in the quantification of surface defects such as those encountered in reinforced concrete bridge decks. Therefore, an efficient self-adaptive segmentation method is developed to detect and classify the image pixels into a distress and a background. The present study explores the effectiveness of modelling the segmentation process as an optimization problem to search for the best threshold values. The present study introduces an exhaustive search multi-objective invasive weed-based optimization method for bi-level thresholding of distress images. The framework of the proposed method involves a two-stage process, whereas five fitness functions are investigated to search for the optimum threshold in the first stage. The five segmentation methods are: Kapur entropy, cross entropy, Ostu function, Tsallis entropy and Renyi entropy. Then, the five segmentation methods are sorted based on mean-squared error, peak signal to noise ratio and structural similarity index. The best two performing segmentation methods are used as an input to design a bi-objective optimization model. Renyi entropy function and Kapur entropy functions are selected as the best two performing methods.

The performance of the bi-objective optimization model is manifested through four levels of comparison. The performance of the developed multi-objective optimization-based method outperformed the single-objective optimization-based methods, which proves the claim that the single-objective optimization-based methods cannot optimally fit all types of images. Then, the proposed method is compared with some conventional segmentation methods such as Otsu method, region growing, K-means clustering, fuzzy C-means clustering, expectation maximization clustering and adaptive thresholding. The average values of the MSE, $PSNR$ and $SSIM$ of the proposed method are equal to 0.0784, 11.4831 and 0.9921, respectively. As such, it is capable of achieving an improvement in the performance of MSE, $PSNR$ and $SSIM$ by 39.225%, 28.999% and 0.558%, respectively when compared to the conventional Otsu method. This highlights that the classical segmentation methods diverge in the case of complex, non-uniform illumination and low contrast images. In order to validate the employment of the invasive weed optimization algorithm, its performance is compared with other metaheuristics such as genetic algorithm, particle swarm optimization algorithm, and harmony search algorithm. The developed multi-objective invasive weed optimization-based method demonstrated better segmentation performance when compared to the multi-objective genetic algorithm-based method, multi-objective particle swarm-based method and multi-objective harmony search-based method. This illustrates the capability of the invasive weed optimization algorithm in providing a superior exploration-exploitation trade-off, which increases the potential of the proposed method to be applied to a wide range of images. Finally, the proposed method is compared with the conventional segmentation methods for a certain number of images to provide an in-depth evaluation of the proposed method and to highlight its consistent superior performance over the segmentation methods. The proposed method yielded better segmentation for the three images. This clarifies the comprehensive, consistent and superior performance of the proposed multi-objective invasive weed optimization-based method. Therefore, the proposed method adopted in the present study can provide better detection and quantification of cracks, which eventually leads to establishing more efficient and reliable condition assessment models.

10 REFERENCES

Abu-Al-Nadi, D. I., Alsmadi, O. M. K., Abo-hammour, Z. S., Hawa, M. F., and Rahhal, J. S. (2013). Invasive Weed Optimization for Model

Order Reduction of Linear MIMO Systems. *Applied Mathematical Modelling*, 37(6), 4570–4577.

Agrawal, S., Panda, R., Bhuyan, S., and Panigrahi, B. K. (2013). Tsallis Entropy Based Optimal Multilevel Thresholding Using Cuckoo Search Algorithm. *Swarm and Evolutionary Computation*, 11, 16–30.

Akay, B. (2013). A Study on Particle Swarm Optimization and Artificial Bee Colony Algorithms for Multilevel Thresholding. *Applied Soft Computing*, 13(6), 3066–3091.

Aziz, M. A. El, Ewees, A. A., and Hassanien, A. E. (2017). Whale Optimization Algorithm and Moth-Flame Optimization for Multilevel Thresholding Image Segmentation. *Expert Systems With Applications*, 83, 242–256.

Azizipour, M., Ghalenoei, V., Afshar, M. H., and Solis, S. S. (2016). Optimal Operation of Hydropower Reservoir Systems Using Weed Optimization Algorithm. *Water Resources Management*, 30(11), 3995–4009.

Banharnsakun, A. (2017). Hybrid ABC-ANN for Pavement Surface Distress Detection and Classification. *International Journal of Machine Learning and Cybernetics*, 8(2), 699–710.

Bhandari, A. K., Kumar, A., and Singh, G. K. (2015). Tsallis Entropy Based Multilevel Thresholding for Colored Satellite Image Segmentation using Evolutionary Algorithms. *Expert Systems With Application*, 42(22), 8707-8730.

Chakraborty, S., Chatterjee, S., Dey, N., Ashour, A. S., Ashour, A. S., and Shi, F. (2017). Modified Cuckoo Search Algorithm in Microscopic Image Segmentation of Hippocampus. *Microscopy Research and Technique*, 1–22.

Felio, G. (2016). Canadian Infrastructure Report Card. Canadian Construction Association, Canadian Public Works Association, Canadian Society for Civil Engineering, and Federation of Canadian Municipalities, Canada. <www.canadainfrastructure.ca/downloads/Canadian_Infrastructure_Report_2016.pdf> (06.05.2016).

Ganesh, M., Naresh, M., and Arvind, C. (2017). MRI Brain Image Segmentation Using Enhanced Adaptive Fuzzy K-Means Algorithm. *Intelligent Automation & Soft Computing*, 23(2), 325–330.

Hammouche, K., Diaf, M., and Siarry, P. (2008). A Multilevel Automatic Thresholding Method Based on A Genetic Algorithm For A Fast Image Segmentation. *Computer Vision and Image Understanding*, 109(2), 163–175.

Hooda, H., and Verma, O. P. (2014). Brain Tumor Segmentation : A Performance Analysis using K-Means , Fuzzy C-Means and Region Growing Algorithm. In *2014 IEEE International Conference on Advanced Communication Control and Computing Technologies (ICACCCT)*. Ramanathapuram, India, 8-10 May.

Horng, M. (2010). A multilevel image thresholding using the honey bee mating optimization. *Applied Mathematics and Computation*, 215(9), 3302–3310.

Hu, J., Li, D., Chen, G., Duan, Q., and Han, Y. (2012). Image Segmentation Method For Crop Nutrient Deficiency Based On Fuzzy C-Means Clustering Algorithm. *Intelligent Automation & Soft Computing*, 18(8), 1145–1155.

Jung, Y., Kang, M., and Heo, J. (2014). Clustering Performance Comparison Using K-means and Expectation Maximization Algorithms. *Biotechnology and Biotechnological Equipment*, 28, S44-S48.

Kaur, D., and Kaur, Y. (2014). Various Image Segmentation Techniques : A Review. *International Journal of Computer Science and Mobile Computing*, 3(5), 809–814.

Keskin, G. A. (2015). Using integrated fuzzy DEMATEL and Fuzzy C : means Algorithm for Supplier Evaluation and Selection. *International Journal of Production Research*, 53(12), 3586-3602.

Khairuzzaman, A. K., and Chaudhury, S. (2017). Multilevel Thresholding using Grey Wolf Optimizer for Image Segmentation. *Expert Systems With Applications*, 86, 64–76.

Khanna, A., Sood, M., and Devi, S. (2012). US Image Segmentation Based on Expectation Maximization and Gabor Filter. *International Journal of Modeling and Optimization*, *2*(3).

Manic, K. S., Priya, R. K., and Rajinikanth, V. (2016). Image Multithresholding based on Kapur / Tsallis Entropy and Firefly Algorithm. *Indian Journal of Science and Technology*, 9(12).

Maru, D., and Shah, B. (2013). Image Segmentation Techniques and Genetic Algorithm. *International Journal of Advanced Research in Computer Engineering and Technology (IJARCET)*, 2(4), 1483–1487.

Mishra, S., and Panda, M. (2018). Bat Algorithm for Multilevel Colour Image Segmentation Using Entropy-Based Thresholding. *Arabian Journal for Science and Engineering*, 43(12), 7285-7314.

Mohammed Abdelkader, E., Marzouk, M., and Zayed, T. (2019). An Optimization-based Methodology For The Definition of Amplitude Thresholds of The Ground Penetrating Radar. *Soft Computing*, 1–24.

Nandy, S., Yang, X., Sarkar, P. P., and Das, A. (2015). Color Image Segmentation By Cuckoo Search. *Intelligent Automation & Soft Computing*, 21(4), 673–685.

National Research Council Canada. (2013). "*Critical Concrete Infrastructure: Extending the Life of Canada's Bridge Network*". <http://www.nrc-cnrc.gc.ca/ci-ic/article/v18n1-5> (20.12.2016).

Oliva, D., Hinojosa, S., Osuna-Enciso, V., Cuevas, E., Pérez-Cisneros, M., and Sanchez-Ante, G. (2019).

Image Segmentation by Minimum Cross Entropy using Evolutionary Methods. *Soft Computing*, 23(2), 431-450.

Oliva, D., Cuevas, E., Pajares, G., Zaldivar, D., and Perez-cisneros, M. (2013). Multilevel Thresholding Segmentation Based on Harmony Search Optimization. *Journal of Applied Mathematics*, Article ID I575414, 24 pages.

Saparudin, E., Nevriyanto, A., and Purnamasari, D. (2018). Performance Analysis of Comparison between Region Growing , Adaptive Threshold and Watershed Methods for Image Segmentation. In *Proceedings of the International MultiConference of Engineers and Computer Scientists*, Hong Kong, 14-16 March.

Sathya, P. D., and Kayalvizhi, R. (2011). Image Segmentation Using Minimum Cross Entropy and Bacterial Foraging Optimization Algorithm. *2011 International Conference on Emerging Trends in Electrical and Computer Technology*, Nagercoil, India, 23-24 March.

Sawant, K. B. (2015). "Efficient Determination of Clusters in K-Mean Algorithm Using Neighborhood Distance". *International Journal of Emerging Engineering Research and Technology*, 3(1), 22–27.

Sennah, K., Juette, B., Witt, C., and Combar, P. M. (2011). Vehicle Crash Testing On a GFRP-Reinforced PL-3 Concrete Bridge Barrier. In *Proceedings of the 4th International Conference on Durability and Sustainability of Fibre Reinforced Polymer Composites for Construction and Rehabilitation*, Québec City, Canada, 20-22 June.

Shedthi, S., Shetty, S., and Siddappa, M. (2017). "Implementation and Comparison of K-Means and Fuzzy C-Means Algorithms for Agricultural Data." *International Conference on Inventive Communication and Computational Technologies*, Coimbatore, India, 10-11 March.

Statistics Canada. (2009). "*Age of Public Infrastructure: A Provincial Perspective*". http://www.statcan.gc.ca/pub/11-621-m/11-621-m2008067-eng.htm> (20.12.2016).

Suresh, S., and Lal, S. (2017). Multilevel Thresholding based on Chaotic Darwinian Particle Swarm Optimization for Segmentation of Satellite Images. *Applied Soft Computing Journal*, *55*, 503–522.

Zhang, Y., and Wu, L. (2011). Optimal Multi-Level Thresholding Based on Maximum Tsallis Entropy via an Artificial Bee Colony Approach. *Entropy*, 13, 841–859.

Zhou, Y.-Q., and Xidian, H. C. (2014). Invasive Weed Optimization Algorithm for Optimization No-Idle Flow Shop Scheduling Problem. *Neurocomputing*, 137, 285–292.

11 NOTES ON CONTRIBUTORS

Eslam Mohammed Abdelkader is a research assistant in Civil Engineering, Concordia University, Canada. He worked as an assistant lecturer in Structural Engineering Department in Cairo University. He received his B.SC and M.SC degrees in Civil Engineering from Cairo University, Egypt in 2012, and 2015, respectively. Eslam received serveral excellence awards.

Osama Moselhi is a professor at Concordia University. He received his BSc. in civil engineering from Cairo University, Egypt in 1970. He obtained the PhD. in structural engineering, Concordia University, Canada in 1978. He held several industrial and academic posts in Canada and abroad in a wide spectrum of the engineering profession.

Mohamed Marzouk is a Professor of Construction Engineering and Management at Department of Structural Engineering, Faculty of Engineering, Cairo University. He received his BSc and MSc in Civil Engineering from Cairo University in 1995 and 1997, respectively. He received his PhD form Concordia University in 2002. He authored and co-authored over 100 scientific publications.

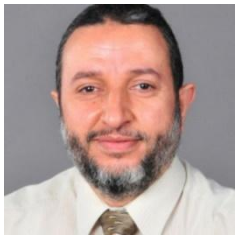

Tarek Zayed has a Ph.D., M.Sc., and B.Sc. in Construction Engineering and Management. He has 30 years of professional experience working in the construction industry training and in academic posts in USA, Canada and abroad. He conducted research in infrastructure management, simulation and artificial intelligence applications in construction.